

OVERVIEW OF THE 6-MV, ROD-PINCH EXPERIMENT ON ASTERIX*

R.J. Comisso⁺, F.C. Young,^a R.J. Allen, D. Mosher, S.B. Swanekamp,^a and G. Cooperstein
Plasma Physics Division, Naval Research Laboratory, Washington, DC 20375; USA

F. Bayol, A. Garrigues, C. Delbos, and G. Nicot
Centre d' Etudes de Gramat, Gramat, France

**C. Vermare, J. Delvaux, Y. Hordé, E. Merle, R. Nicolas, D. Noré, O. Pierret, Y.R. Rosol,
Y. Tailleur, and L. Véron**
Polygone d'Expérimentation de Moronvilliers, Moronvilliers, France

B.V. Oliver,^b D.V. Rose,^b D. Rovang, D.L. Johnson,^c J. Maenchen, and K. Prestwich^d
Sandia National Laboratories, Albuquerque, NM 87185, USA

Abstract

This work presents the highlights of high-voltage, positive-polarity experiments on the ASTERIX generator characterizing the rod-pinch diode at up to 6 MV as a source for high-resolution, flash radiography. The paper reviews experimental results and analyses including conversion of ASTERIX to positive polarity, rod-pinch electrical and radiation characteristics, comparisons to numerical simulation, and composite rod-pinch performance. A minimum LANL source diameter of 1.32 mm with a dose of 23.7 rad(air) at 1 m was achieved at a peak voltage of 5.9 MV, leading to a radiographic figure-of-merit of 13.6 rad(Si)/mm². The results demonstrate the utility of the rod pinch for high-power pulsed radiography at up to 6 MV.

I. INTRODUCTION AND SETUP

The rod-pinch (RP) diode [1,2] has previously been evaluated as a radiation source for high-power flash radiography at the 1- to 2-MV level on Gamble II [3] and Sabre [4], and at the 2- to 4-MV level on ASTERIX (ASTERIX-1) [5-7]. The current work is focused on characterizing the rod-pinch diode at up to 6 MV, again using ASTERIX but modified for higher-voltage operation in positive polarity (ASTERIX-2). [8-10] Radiation diagnostics were expanded to provide a detailed angular distribution of the dose between 0° (on-axis) and 90°, and the source radiation distribution at 0° and 90°. In this paper, the highlights of the experimental results and analyses, including conversion to positive polarity, RP electrical and radiation characteristics, and the composite-

rod-pinch (CRP) diode [3,5,6] results are reviewed. The companion papers in these proceedings provide detailed results on the radiographic characteristics and dose angular distribution [8], CRP operation and source axial radiation distribution [9], and numerical simulation [10].

The CEG ASTERIX generator [11] consists of a 64-stage, 6.4-MV (erected), 192-kJ Marx driving a 35-Ω oil Blumlein. A schematic illustrating the major components of ASTERIX generator is given in Fig. 1. Oil and vacuum prepulse switches [12] combine to reduce the bipolar prepulse across the diode to about +16 kV and -8 kV at 90-kV Marx charge. [7,8] A voltage divider located across the insulator is used to infer the voltage at the load by inductive correction. Current is measured with B-dot loops (not shown) located between the insulator stack and door on the 1.05-m-ID vacuum chamber.

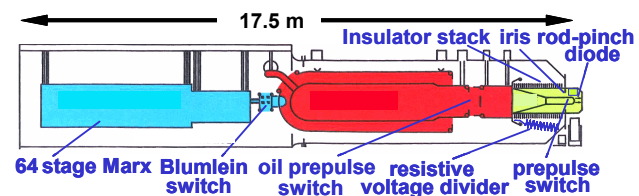


Fig. 1. Schematic illustration of ASTERIX.

A drawing of the RP load region is shown in Fig. 2. A 6.4-mm-diam carbon rod extends 22 to 162 mm from the anode stalk, depending on the Marx charge, where it connects to a smaller-diameter W or Au anode rod. The rod projects through an annular carbon (or carbon-coated Al) cathode and usually extends 16 mm beyond it, ending in

* Work supported by the Commissariat à l'Énergie Atomique/DAM, Centre d' Etudes de Gramat/DGA, and Sandia National Laboratories/DOE

⁺ email: comisso@suzie.nrl.navy.mil

^a Titan-JAYCOR Division, McLean, VA 22101

^b Mission Research Corporation, Albuquerque, NM 87110

^c Titan-Pulse Science Division, San Leandro, CA 94577

^d Prestwich Consultants, Albuquerque, NM, 87185

Report Documentation Page

Form Approved
OMB No. 0704-0188

Public reporting burden for the collection of information is estimated to average 1 hour per response, including the time for reviewing instructions, searching existing data sources, gathering and maintaining the data needed, and completing and reviewing the collection of information. Send comments regarding this burden estimate or any other aspect of this collection of information, including suggestions for reducing this burden, to Washington Headquarters Services, Directorate for Information Operations and Reports, 1215 Jefferson Davis Highway, Suite 1204, Arlington VA 22202-4302. Respondents should be aware that notwithstanding any other provision of law, no person shall be subject to a penalty for failing to comply with a collection of information if it does not display a currently valid OMB control number.

| | | | |
|--|------------------------------------|--|--|
| 1. REPORT DATE JUN 2003 | 2. REPORT TYPE N/A | 3. DATES COVERED - | |
| 4. TITLE AND SUBTITLE Overview Of The 6-Mv, Rod-Pinch Experiment On Asterix | | 5a. CONTRACT NUMBER | |
| | | 5b. GRANT NUMBER | |
| | | 5c. PROGRAM ELEMENT NUMBER | |
| 6. AUTHOR(S) | | 5d. PROJECT NUMBER | |
| | | 5e. TASK NUMBER | |
| | | 5f. WORK UNIT NUMBER | |
| 7. PERFORMING ORGANIZATION NAME(S) AND ADDRESS(ES) Plasma Physics Division, Naval Research Laboratory, Washington, DC 20375; USA | | 8. PERFORMING ORGANIZATION REPORT NUMBER | |
| 9. SPONSORING/MONITORING AGENCY NAME(S) AND ADDRESS(ES) | | 10. SPONSOR/MONITOR'S ACRONYM(S) | |
| | | 11. SPONSOR/MONITOR'S REPORT NUMBER(S) | |
| 12. DISTRIBUTION/AVAILABILITY STATEMENT Approved for public release, distribution unlimited | | | |
| 13. SUPPLEMENTARY NOTES See also ADM002371. 2013 IEEE Pulsed Power Conference, Digest of Technical Papers 1976-2013, and Abstracts of the 2013 IEEE International Conference on Plasma Science. IEEE International Pulsed Power Conference (19th). Held in San Francisco, CA on 16-21 June 2013. U.S. Government or Federal Purpose Rights License, The original document contains color images. | | | |
| 14. ABSTRACT This work presents the highlights of high-voltage, posi-tive-polarity experiments on the ASTERIX generator characterizing the rod-pinch diode at up to 6 MV as a source for high-resolution, flash radiography. The paper reviews experimental results and analyses including con-version of ASTERIX to positive polarity, rod-pinch elec-trical and radiation characteristics, comparisons to nume-rical simulation, and composite rod-pinch performance. A minimum LANL source diameter of 1.32 mm with a dose of 23.7 rad(air) at 1 m was achieved at a peak voltage of 5.9 MV, leading to a radiographic figure-of-merit of 13.6 rad(Si)/mm2. The results demonstrate the utility of the rod pinch for high-power pulsed radiography at up to 6 MV. | | | |
| 15. SUBJECT TERMS | | | |
| 16. SECURITY CLASSIFICATION OF: | | | 17. LIMITATION OF ABSTRACT SAR |
| a. REPORT unclassified | b. ABSTRACT unclassified | c. THIS PAGE unclassified | |
| | | | 18. NUMBER OF PAGES 4 |
| | | | 19a. NAME OF RESPONSIBLE PERSON |

either a blunt or tapered (10 mm to a point) tip. [8,9] Anodes of 1.0- 1.6-, 2.0-, and 3.0-mm diam are used, and the initial ratio of the cathode-to-anode radius, R_C/R_A , ranges from 11 to 20. [8] Several CRP diode designs were also tested: a hollow aluminum tube (1.96-mm OD/1.4-mm ID) replaces the W or Au anode and supports either a 1-cm-long, 1-mm-diam Au insert (blunt or tapered) or a 1.5- to 2-mm-diam Au sphere. [9] The power feed gap (see Fig. 2) is usually set to 20 cm for 90-kV Marx charge and reduced for lower charging voltages. [12] Four B-dots measure the current in proximity to the RP. These B-dot measurements agree with the current measured upstream at the vacuum chamber location. The dose and its time history are measured at various angular locations using LiF TLDs and Si *pin* diodes. [8] Measurements of the radiation distribution at the source are made using 82-cm-radius, W rolled-edges located at 0° and 80°. [8,9]

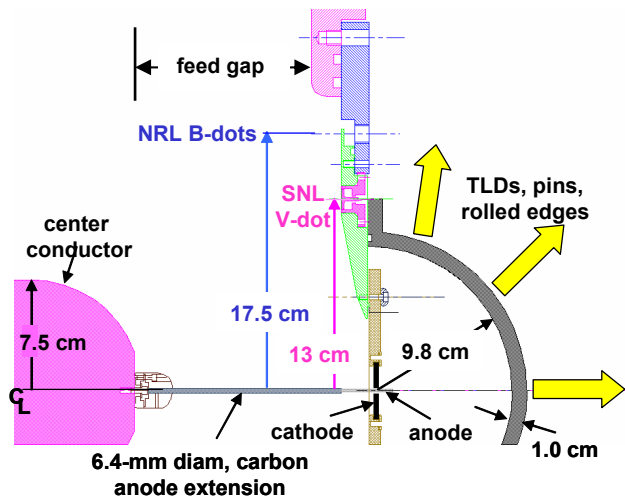


Fig. 2. Illustration of rod-pinch diode region.

II. POLARITY REVERSAL

For the 4-MV RP experiments [5-7], minor modifications were made to ASTERIX. [12] To explore the 6-MV regime, additional modifications and analyses were required. 1) The Blumlein oil switch had been designed to have equal breakdown probability from either electrode in negative polarity by enhancing the negative electrode. For positive polarity, the electrodes are physically reversed to maintain the same breakdown symmetry and a similar relationship between gap spacing and voltage. 2) New electrostatic plots and analysis were done on all polarity-dependent field-enhanced regions of the Blumlein transmission lines. The probability of breakdown in the region of highest electric field (on the end of the Blumlein intermediate cylinder) at 90-kV Marx charge (compared with the usual value of 85 kV in negative polarity) is about 3%. 3) The insulator stack is reconfigured by reversing the direction of the 45° bevel on the insulator rings, anodizing the grading rings, and anodizing and increasing the diameter of the field shaping “iris” (see Fig. 1., also used to protect the stack from debris). The latter two changes are implemented to prevent electron emission from the

rings and the iris, which are at negative high voltage in positive polarity. With 7.5 MV across the stack (93-kV Marx charge), electric fields on the grading rings are about 300 kV/cm. Parallel electric fields at the cathode triple points are checked to comply with the usual design criterion of 30 kV/cm. An inverse e-beam diode was designed, fabricated, and used for the positive-polarity pulsed-power tests. More than 7.5 MV was supported across the insulator stack during these successful tests.

III. DIODE ELECTRICAL BEHAVIOR

Typical time histories for the load voltage (V), load current (I), and impedance ($Z = V/I$) for the RP on shot 7165 (90-kV Marx charge) are shown in Fig. 3. A tapered, 2-mm-diam W anode rod with $R_C/R_A = 16$ is used. The voltage is determined by applying an inductive correction to the voltage measured at the insulator stack. Although the large inductance (1030 nH) separating the voltage divider and load can result in up to a 20% correction, and the voltage- and current-measurement locations are separated by about 6 to 7 ns (one-way), the voltage so determined agrees reasonably well with that inferred from the radiation (see below and [10]). Near the time of peak radiation, $V \approx 5.9$ MV, $I \approx 105$ kA, and $Z \approx 55 \Omega$.

The measured 20° *pin* diode trace in Fig. 3 is compared with $IV^{1.25}$, normalized to the *pin* signal. The exponent of 1.25 is from coupled PIC and electron-photon transport calculations of dose-rate at 20°. [10] Similar agreement between measured dose rate and electrical parameters in radiation shape and absolute magnitude is found at all angles investigated over a range of diode parameters. [10] Based on this agreement, the quoted voltage near the time of peak radiation is accurate to within $\pm 10\%$.

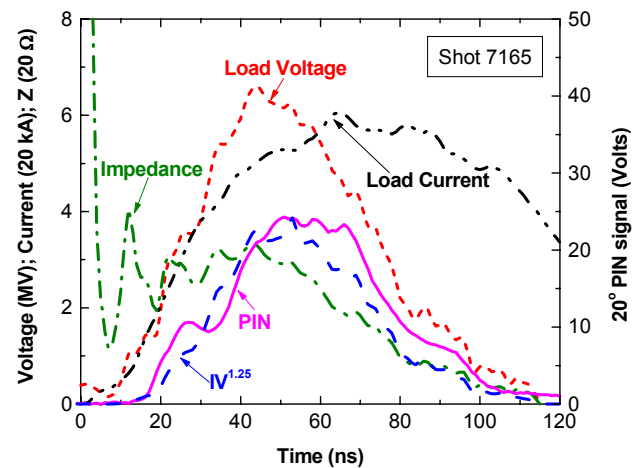


Fig. 3. Load voltage, current, and impedance, and the *pin* signal at 20° compared with $IV^{1.25}$.

The behavior described above is typical of diodes with 1.6- to 3.0-mm-diam anodes and initial $R_C/R_A \leq 16$, independent of anode material. For a 1-mm-diam anode and $R_C/R_A = 16$, lower voltage and rapid impedance collapse are observed. Small diameter anodes naturally exhibit faster impedance collapse because electrode-plasma

expansion during the pulse represent a larger fraction of the initial anode radius. For a fixed R_C/R_A , smaller-radius anodes have proportionately smaller AK gaps ($R_C - R_A$), leading to enhanced prepulse effects. [8,9] In addition, enhanced e-beam heating of a smaller-radius rod may result in a higher rate of anode-plasma expansion.

Hardware in the diode region is radioactive after a shot because protons in the system acquire kinetic energy associated with the diode voltage. The half-lives of the radioactivity associated with the carbon cathode and aluminum end-plate were measured. The carbon cathode decays with a 10-min half-life consistent with ^{13}N decay. This activity can be produced by proton-induced reactions on carbon: the $^{12}\text{C}(p,\gamma)^{13}\text{N}$ reaction which has a low-energy resonance at 0.46 MeV, and the $^{13}\text{C}(p,n)^{13}\text{N}$ reaction with a 3.0-MeV threshold energy. [13] The aluminum end-plate has a 38-min half-life consistent with ^{63}Zn decay. This activity can be produced by the $^{63}\text{Cu}(p,n)^{63}\text{Zn}$ reaction, with a 4.2-MeV threshold energy on the 4% Cu impurity in type 2017 aluminum. The radioactivity measurements indicate that diode voltages ≥ 4 MV are produced.

IV. SOURCE CHARACTERISTICS

Figure 4 shows dose on axis 1 m from the source for 2-mm-diam tapered W anodes, normalized to the integral of the load current (Q) as a function of the average voltage during the time that the 20° pin diode is within 80% of maximum. Lower-voltage shots are from ASTERIX-1. The best fit to a power law results in a $V^{1.24}$ normalized-dose scaling. This scaling agrees with the on-axis dose-rate/ I scaling from simulations [10,14], but is weaker than

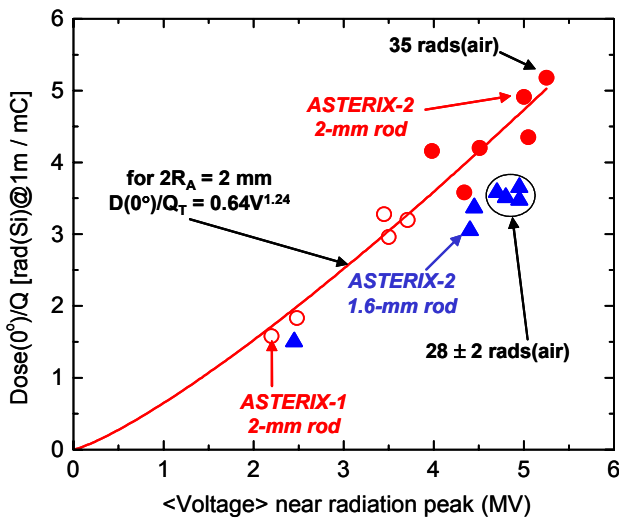


Fig. 4. Dose normalized to charge as a function of average voltage for 2.0- and 1.6-mm-diam anodes.

observed on ASTERIX-1 [5-7] and Gamble II [3]. Simulations [10,14] show that as the voltage increases, electron angles of incidence at the rod tip are more backward directed. For fixed voltage, the dose is reproducible to $\pm 6\%$. As the voltage is increased to 6 MV, 2-mm-diam rods make more radiation than 1.6-mm-diam rods, similar

to lower-voltage ASTERIX-1 results with 1-mm-diam rods. [5-7] This could be a result of insufficient mass to effectively absorb the electron beam near the rod tip.

As shown in Fig. 5, the dose exhibits an anisotropy in angle, with the dose at 80° being 1.6 to 1.8 times higher than on axis. [8-10] This trend is reproduced by simulation [10, 14] and is again a result of the electron angles of incidence being more backward directed at higher voltage. For high voltage, a negative-polarity geometry might better utilize the natural electron directionality to maximize the forward-directed dose. [10, 15]

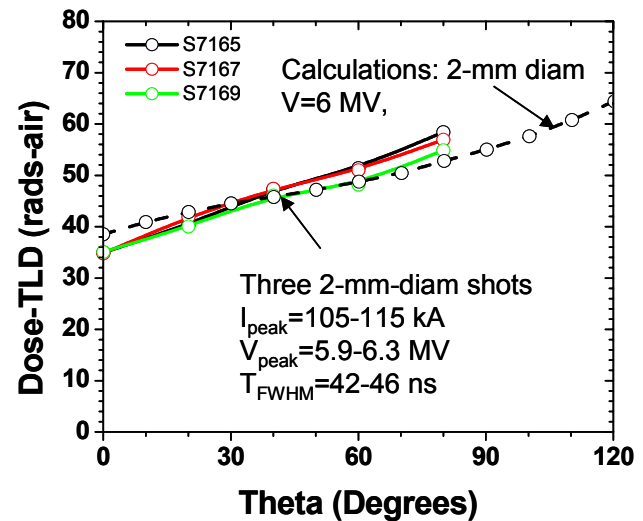


Fig. 5. Measured dose as a function of angle, compared with simulation results.

For the highest dose shot, 35 rad(air) at 1 m (6.3-MV peak), the LANL definition source diameter (50% point of the MTF), SD, is 1.95 mm, giving a radiographic figure-of-merit (FOM) [(dose at 1 m)/(source size) 2] of 9.2 rad(air)/mm 2 . While the dose is fairly insensitive to anode material or tip geometry (tapered or blunt), the SD and axial radiation distribution are quite different for blunt and tapered rods, again a result of the electron trajectories at the tip of the rod. [9]

V. COMPOSITE RP DIODE

The composite diode is designed to avoid rapid impedance decay for small (≤ 1 -mm-diam) anodes. A larger-diameter, low-Z anode extends through the cathode while keeping R_C/R_A about constant, thus increasing ($R_C - R_A$). Rapid and efficient e-beam propagation along this hollow anode from the cathode to a smaller-diameter, solid high-Z tip maintains small source size and high dose. With larger R_A , the specific energy deposition in the anode and the fractional change in R_A over time from plasma expansion are reduced. For the optimum configuration in this experiment, the W or Au anode rod is replaced with a 1.96-mm OD/1.4-mm ID Al tube supporting a 1-cm-long, 1-mm-diam tapered Au slug. [9] This geometry results in a dose at 1 m of 23.7 rad(air) (5.9-MV peak) with an SD of 1.32 mm, and gives the highest FOM achieved in this

work of $13.6 \text{ rad(air)/mm}^2$. The line-spread function (LSF) for this case is shown in Fig. 6, along with that calculated for a 1.6-mm base-diameter uniformly-emitting cone. [9] For both standard RP and CRP diodes at fixed diode conditions, the SD is reproducible to about $\pm 5\%$.

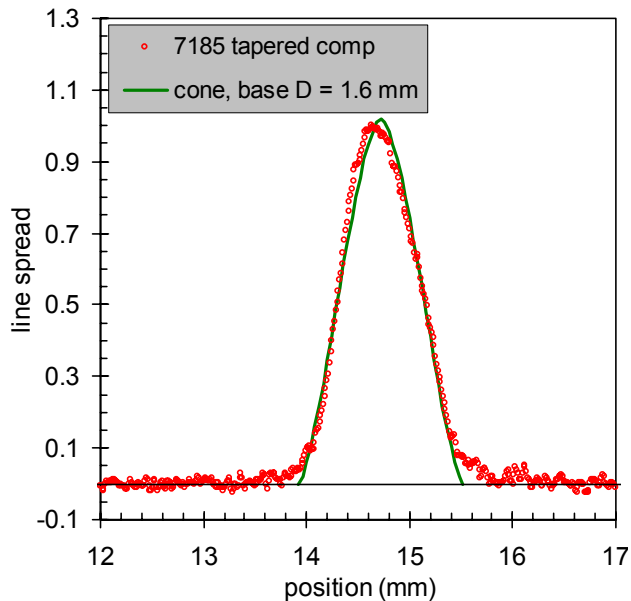


Fig. 6. Measured LSF for CRP shot 7185, compared with calculated LSF. The LANL SD is 1.32 mm.

VI. SUMMARY

In summary, the rod-pinch diode is characterized as a source for high-resolution, flash radiography at up to 6 MV using the ASTERIX generator, modified for high-voltage, positive-polarity operation. Good electrical behavior is observed for RP diodes with anodes having 1.6-, 2.0-, or 3.0-mm diam and initial $R_C/R_A \leq 16$ (independent of anode material). For the case of a 1-mm-diam anode and $R_C/R_A = 16$, lower voltage and rapid impedance collapse are observed. The normalized dose scales as $V^{1.24}$ and the dose at 80° is 1.6 to 1.8 times higher than on axis, in agreement with simulations. Using a CRP diode, a minimum LANL spot-size of 1.32 mm with a dose of 23.7 rad(air) at 1 m is achieved, resulting in the highest FOM of 13.6. These results demonstrate that the rod pinch is a useful source for high-power pulsed radiography at up to 6 MV. For high-voltage operation, a negative-polarity geometry might better utilize the natural electron directionality to maximize the dose on axis.

VII. REFERENCES

- [1] S.B. Swanekamp, et al., "Particle-in-cell Simulations of High-Power Cylindrical Electron Beam Diodes," *Phys. Plasmas* **7**, pp. 5214-5222, 2000.
- [2] G. Cooperstein, et al., "Theoretical Modeling and Experimental Characterization of a Rod-Pinch Diode," *Phys. Plasmas* **9**, pp. 4418-4636, 2001, and references therein.
- [3] R.J. Commisso et al., "Experimental Evaluation of a Megavolt Rod-Pinch Diode as a Radiography Source," *IEEE Trans. Plasma Sci.* **30**, pp. 338-350, 2002.
- [4] P.R. Menge, et al., "Optimization of a Rod-Pinch Diode Radiography Source at 2.3 MV," *Rev. Sci. Instrum.* **74**, August 2003, to be published.
- [5] F. Bayol et al., "Evaluation of the rod-pinch diode as a high resolution source for flash radiography at 2 to 4 MV," in *Proc. Pulsed Power Plasma Science 2001 Conf.*, R. Reinovsky and M. Newton, Eds., Piscataway, NJ: IEEE, 2001, vol. 1, pp. 450-453.
- [6] R.J. Commisso et al., "Characterization of the Rod-Pinch Diode at 2 to 4 MV as a High-Resolution Source for Flash Radiography," *AIP Conf. Proc.* **650**, 2002, pp. 183-186.
- [7] F.C. Young et al., "Rod-Pinch Diode Operation at 2 to 4 MV for High Resolution Radiography," *Phys. Plasmas* **9**, pp. 4815-4818, 2002.
- [8] F.C. Young, et al., these proceedings.
- [9] D. Mosher et al., these proceedings.
- [10] S. Swanekamp et al., these proceedings.
- [11] G. Raboison, et al., "ASTERIX, A High Intensity X-Ray Generator," in *Proc. Int. Pulsed Power Conf.* - 1989, B.H. Bernstein and J.P. Shannon, Eds., New York, NY: IEEE, 1989, pp. 567-570.
- [12] R.J. Allen, et al., "Adaptation of Asterix to a Positive Polarity for 2 to 4 MV Rod-Pinch Diode Experiments and Diode Electrical Analysis," in *Proc. Pulsed Power Plasma Science 2001 Conf.*, op. cit., pp. 446-449.
- [13] F.C. Young and D.V. Rose, *Atomic Data and Nuclear Data Tables* **64**, pp. 223-252, 1996.
- [14] D.V. Rose, "Coupled particle-in-cell and Monte Carlo transport modeling of intense radiographic sources," *J. Appl. Phys.* **91**, pp. 3328-3335, 2002.
- [15] G. Cooperstein, et al., these proceedings